Effects of Particle Shape on the Effective Permittivity of Composite Materials With Measurements for Lattices of Cubes

Keith W. Whites, *Senior Member, IEEE*, and Feng Wu

***Abstract*—The effects of inclusion shape on the quasi-static effective permittivity of a two-phase periodic composite material are discussed in this paper. The lattice is formed from complex-shaped conducting inclusions suspended in a host medium. The effective permittivity is computed using an accurate moment-method-based technique. Numerical results are presented for a variety of particle shapes including circular, square, and "rounded square" cylinders (two dimensional) as well as lattices of spheres and cubes (three dimensional). It was found that among these shapes, lattices of square cylinders and cubes produced nearly the minimal polarization per unit volume possible (à la Maxwell/Maxwell Garnett). It appears that the strong mutual interaction between edges and corners of these particles is responsible for this effect. That is, it was observed that the mutual interaction between square cylinders and cubes caused a decrease in their dipole moments and, hence, the effective permittivity, which is opposite to the usual expectation from mutual interaction between circular cylinders and spheres. Experimental verification of this effect is provided by quasi-static conductivity measurements using an apparatus that simulates an infinite lattice of highly conducting cubes. The methodology and results described in this work can be used to design certain microwave composite materials composed of periodic conductor/dielectric composites.**

***Index Terms*—Complex composite materials, conductivity, dielectric enhancement and reduction, effective permittivity, quasistatic conductivity measurements.**

I. Introduction

VARIOUS applications have been proposed for composite materials constructed of conducting or dielectric inclusions in a host medium. For example, applications for high-dielectric thin-film capacitors and substrates have been suggested [1], [2]. In both cases, an accurate quasi-static effective permittivity is desirable for these materials. However, the analytical analysis of these, and other, composite materials is strictly limited because the scattering and mutual interaction between the inclusions are very complicated to describe. Only a few canonical shapes can be solved accurately using semianalytical techniques such as the T-matrix method [3]. For the complex-shaped inclusions discussed in this paper, we will employ another computational electromagnetics technique. We note that a few methods have been proposed for computing effective material constants for complex-shaped inclusions [2], [4], but the effects of particle shape on the effective permittivity have not been illustrated.

In this paper, we will focus on the effects of inclusion shape on the quasi-static effective permittivity of an infinite lattice containing identical conducting particles. This will be performed both for lattices of two-dimensional (2-D) and three-dimensional (3-D) particles. This accurate numerical analysis is accomplished using a simple method of moments (MM) technique. With this method, the electric potential integral equation is first constructed using the surface equivalence theorem. We then use the MM to solve for the charge distribution on the inclusions for a uniform, but otherwise arbitrary, electric field excitation. The electric dipole moments of the inclusions are then determined from which the effective permittivity of the composite material is calculated through an appropriate macroscopic model.

II. Integral Equation Formulation and Dipole Moment Solution

Consider an infinite lattice of conducting particles suspended in a host medium with permittivity ε_b as shown in Fig. 1(a). This lattice is illuminated by a uniform, but otherwise arbitrary, incident electric field $\mathbf{E}^{\mathrm{inc}}$. Each unit cell contains one charge-neutral conducting particle with a possibly very complicated shape. The lattice, however, is assumed to possess enough symmetry so it is effectively isotropic.

According to the surface equivalence theorem [5], an equivalent electrostatic problem can be constructed where an equivalent surface charge density ρ_s exists on each inclusion i, as shown in Fig. 1(b). The scattered potential from these equivalent sources plus the incident potential produce the total potential Φ^t_{ext} in the region exterior to all particles and a constant potential $\Phi_{c,\,i}$ within particle i $(i=1,\,\ldots,\,\infty)$. Due to the infinite nature of the geometry and the uniform $\mathbf{E}^{\mathrm{inc}}$, ρ_s on each particle must be identical. Furthermore, since the interior null field regions can be replaced by any material without disturbing the value $\mathbf{E}=0$, we will replace them with ε_b.

To compute ρ_s, we apply the constant potential boundary condition in the equivalent problem. That is, the total potential when

Manuscript received March 6, 2001. This work was supported by the National Science Foundation under Faculty Early Career Development (CAREER) Award ECS-9624486.

K. W. Whites is with the Department of Electrical and Computer Engineering, South Dakota School of Mines and Technology, Rapid City, SD 57701 USA (e-mail: whites@sdsmt.edu).

F. Wu is with the Department of Electrical and Computer Engineering, University of Kentucky, Lexington, KY 40506 USA (e-mail: fengwu@engr.uky.edu).

Publisher Item Identifier 10.1109/TMTT.2002.800422.

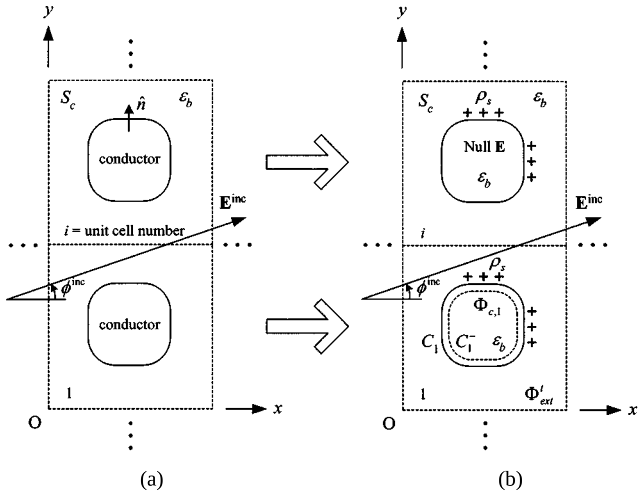

Fig. 1. Geometry of the original problem—containing an infinite lattice of conducting particles immersed in a uniform quasi-static electric field—and the corresponding (external) equivalent problem used in the MM solution. (a) Original problem. (b) Equivalent problem.

evaluated at an observation point $\mathbf{r}_1$ located on surface C_1^- just inside particle 1 must equal $\Phi_{c,1}$ as

$$\Phi^{\rm inc}(\mathbf{r}_1) + \sum_{i=1}^{\infty} \Phi_i^s(\mathbf{r}_1|\varepsilon_b, \rho_s) = \Phi_{c,1}, \qquad \mathbf{r}_1 \in C_1^- \tag{1}$$

where the first term in (1) is the incident potential at $\mathbf{r}_1$ and the second is the scattered potential due to all equivalent sources (particles) in the lattice. In addition, we require that

$$\begin{cases} \oint_{C_1} \rho_s \, dl' = 0, & \text{2-D} \\ \oiint_{S_1} \rho_s \, ds' = 0, & \text{3-D} \end{cases} \tag{2}$$

is enforced so that all particles remain charge neutral, as assumed earlier.

We will use the MM to solve (1) and (2) for ρ_s in both lattices of 2-D and 3-D particles. For a 2-D geometry, the inclusions in the lattice are infinitely long, parallel cylinders with possibly a complicated cross-sectional shape. The scattered potential produced by ρ_s in a 2-D homogeneous space (ε) is [6]

$$\Phi_i^s(\mathbf{r}|\varepsilon, \rho_s) = -\frac{1}{2\pi\varepsilon} \oint_{C_i} \rho_s \ln R_i \, dl'. \tag{3}$$

A pulse-expansion-point-match moment method technique was used to solve this integral equation where the contour of each cylinder was approximated by a number of straight segments L_n $(n = 1, \ldots, N)$ each of length l_n.

After pulse expansion of the charge density and then point matching the discretized integral equation at the centroid of each segment, we can express (1) and (2) in the matrix form

$$\begin{bmatrix} [Z_{mn}]_{N\times N} & [1]_{N\times 1} \\ [l_n]_{1\times N} & 0 \end{bmatrix} \begin{pmatrix} [\alpha_n]_{N\times 1} \\ \Phi_{c,1} \end{pmatrix} = \begin{pmatrix} [\Phi^{\rm inc}(\mathbf{r}_1)]_{N\times 1} \\ 0 \end{pmatrix} \tag{4}$$

where

$$Z_{mn} = \frac{1}{2\pi\varepsilon_b} \sum_{i=1}^{M} \int_{L_n} \ln R_{mn} \, dl' \tag{5}$$

and α_n are the unknown surface charge density coefficients. The elements in (5) are evaluated at the centroid of segment m on C_1^- and the infinite summations have been truncated to M cylinders. As will be shown in Section IV, this simple pulse-expansion-point-match MM solution can provide very accurate quasi-static $\varepsilon_{r,\rm eff}$ calculations for complex composite materials.

The surface charge density of 3-D particles in an infinite lattice can be computed similarly except for the use of triangular patches in the moment method solution. The matrix equation in this case has the same form as (4), except, among other things, (5) becomes

$$Z_{mn} = -\frac{1}{4\pi\varepsilon_b} \sum_{i=1}^{M} \iint_{S_n} \frac{1}{R_{mn}} \, ds' \tag{6}$$

where S_n is the surface of the nth flat triangular patch.

Lastly, once ρ_s has been accurately computed for either 2-D or 3-D lattices, the electric dipole moment $\mathbf{p}$ of each particle can be determined from the numerical solution to (4) as [7], [8]

$$\mathbf{p} = \begin{cases} \oint_{C_i} \rho_s \mathbf{r}' \, dl', & \text{2-D} \\ \oiint_{S_i} \rho_s \mathbf{r}' \, ds', & \text{3-D.} \end{cases} \tag{7}$$

III. Effective Permittivity Computation

A suitable macroscopic model must be chosen in order to compute the effective permittivity of the infinite lattice. The model applied here is that of an arbitrarily large dielectric circular cylinder (2-D) or dielectric sphere (3-D) of relative permittivity $\varepsilon_{r,\rm eff}$ illuminated by the same uniform electric field as in the MM solution [7]. In both instances, the polarization vector is uniform throughout the objects, which is the desired outcome here (in the macroscopic sense) for the infinite lattices.

In the case of a 2-D infinite lattice, the effective relative permittivity is related to the electric dipole moment p of every cylinder through the expression [9]

$$\varepsilon_{r,\rm eff} = 1 + 2\,\frac{\frac{p}{2\varepsilon_0 E^{\rm inc} S_c}}{1 - \frac{p}{2\varepsilon_0 E^{\rm inc} S_c}} \tag{8}$$

where S_c is the cross-sectional area of one unit cell and p is the dipole moment of each cylinder. Similarly, $\varepsilon_{r,\rm eff}$ for 3-D lattices of particles illuminated by a uniform electric field is [7]

$$\varepsilon_{r,\rm eff} = 1 + 3\,\frac{\frac{p}{3\varepsilon_0 E^{\rm inc} V_c}}{1 - \frac{p}{3\varepsilon_0 E^{\rm inc} V_c}} \tag{9}$$

where V_c is the volume of a unit cell.

IV. Results and Discussion

Before presenting $\varepsilon_{r,\rm eff}$ data illustrating the effects of particle shape, we will first subject this solution methodology to verifica-

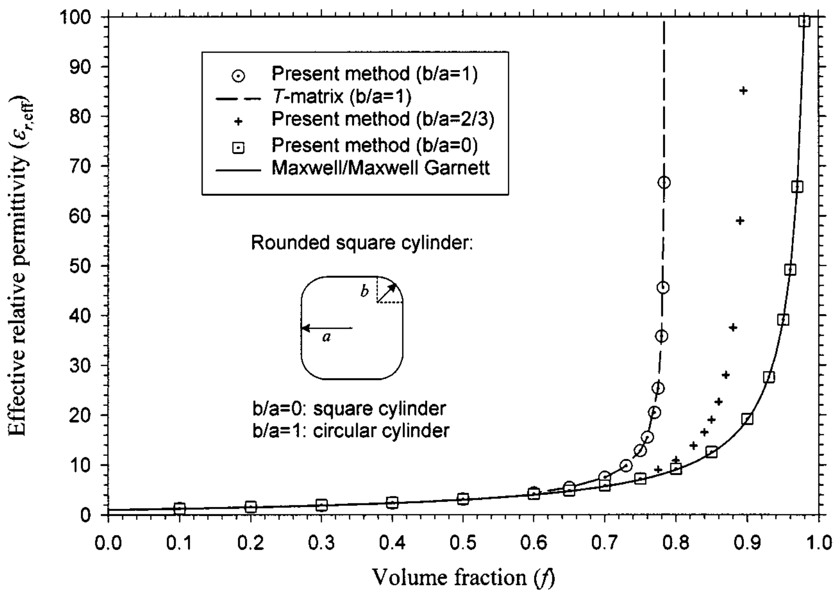

Fig. 2. Computed $\varepsilon_{r,\,\text{eff}}$ for three 2-D conducting particle shapes (circle, rounded square, and square cylinders). Also shown are the T-matrix results for circular conducting cylinders [9]. The Maxwell/Maxwell Garnett (MG) results indicate the lower bound for the static permittivity of these three composite materials.

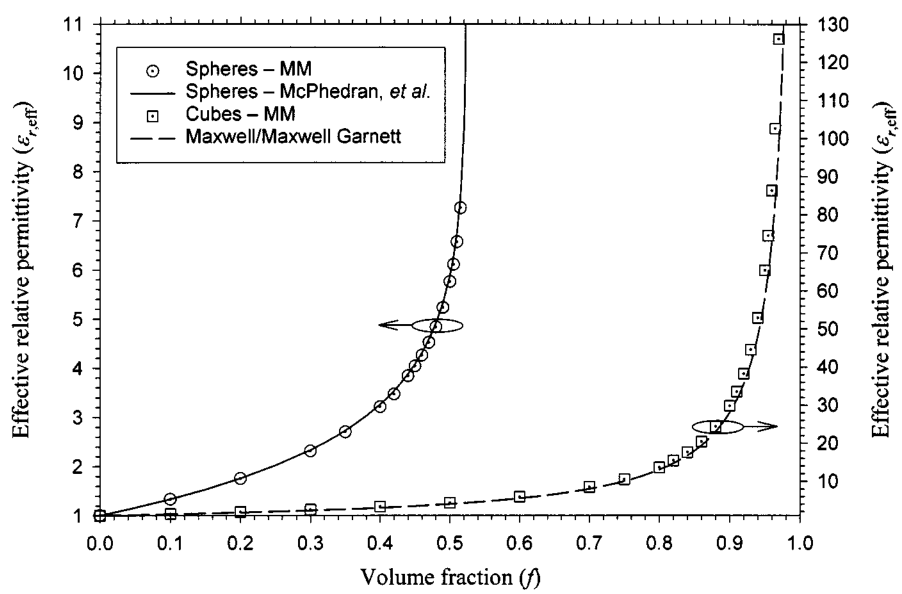

Fig. 3. Computed $\varepsilon_{r,\,\text{eff}}$ for 3-D lattices of conducting spheres and conducting cubes. Our MM solution for conducting spheres is compared with data from [10]. Note that the vertical $\varepsilon_{r,\,\text{eff}}$ scales for the sphere and cube data are much different.

tion. In Figs. 2 and 3, the computed $\varepsilon_{r,\,\text{eff}}$ for conducting circular cylinders and spheres, respectively, are compared with known accurate results (i.e., our semianalytical T-matrix results [7], [9] and those of McPhedran, *et al.* [10]). In both cases, the background is free space ($\varepsilon_b = \varepsilon_0$). The conducting circular cylinders in Fig. 2 form a 2-D square lattice while the conducting spheres in Fig. 3 form a 3-D simple cubic lattice. The excellent agreement in these two comparisons serves as a verification of our method in that the 2-D MM and T-matrix results are very close for all volume fractions (less than approximately 0.75% variation) while the 3-D MM results generally vary by less than 2% from those of McPhedran, *et al.* (at the maximal volume fraction the variation is 3.1%). The MM results were generated using up to $N =$ 360 basis functions in 2-D and 1968 basis functions in 3-D while the maximum number of particles truncated from the infinite lattice, M, was 177 in 2-D and 125 in 3-D. Actually, only within a small range of f close to the maximum do these "large" N and M figures need to be employed. Otherwise, the required number of basis functions and the number of particles in the truncated lattice can be much lower.

Also shown in Figs. 2 and 3 are $\varepsilon_{r,\,\text{eff}}$ for lattices of conducting square cylinders (2-D) and cubes (3-D) computed using our MM-based technique discussed earlier as well as the MG predictions [11, Arts. 314 and 430]. The N, M and ε_b parameters were unchanged from the previous 2-D example whereas for the cube results up to $N = 3758$ basis and $M = 729$ particles were needed near the maximal volume fraction (but considerably smaller N and M otherwise).

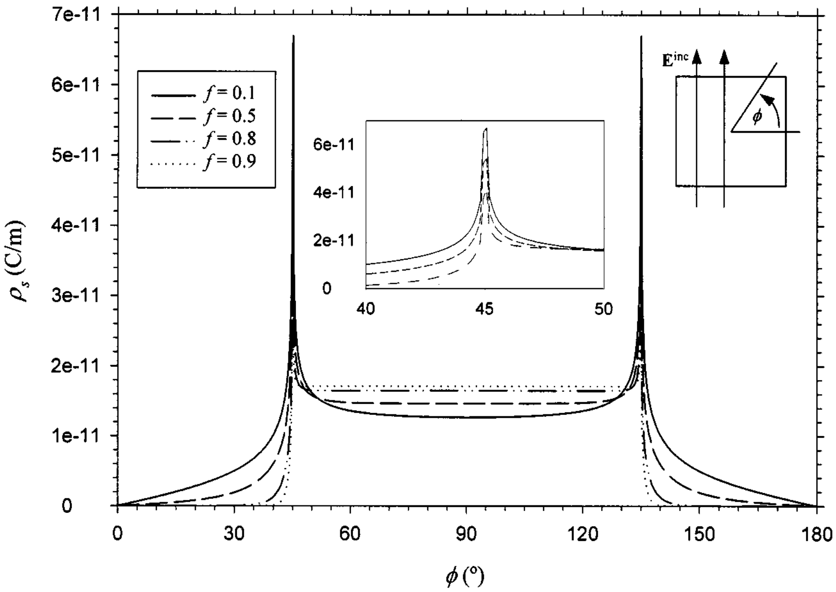

Fig. 4. Surface charge distribution on square conducting cylinders for various volume fraction f ranging from 0.1 to 0.9. The incident field has $E^{\rm inc} = 1$ V/m and $\phi^{\rm inc} = 90°$.

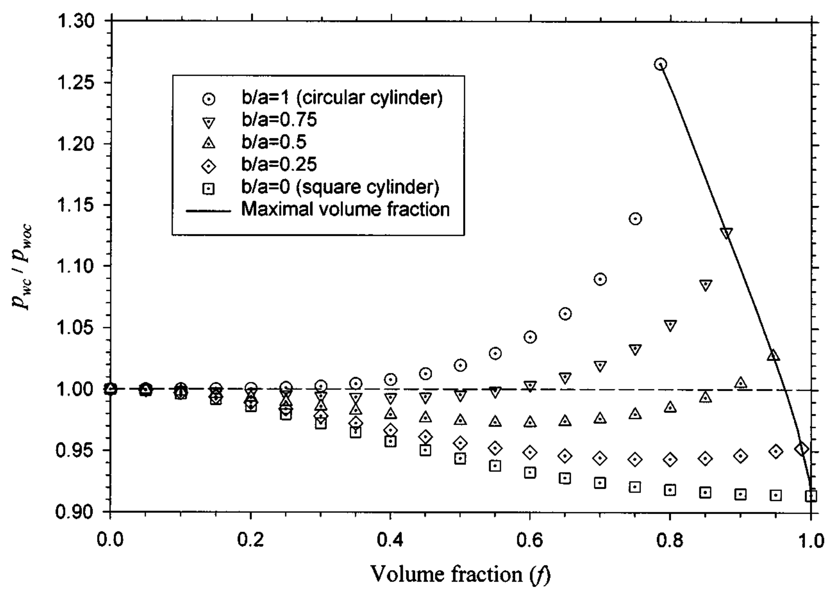

Fig. 5. Ratio of electric dipole moments in the direction of $\mathbf{E}^{\rm inc}$ with mutual coupling ($p_{\rm wc}$) and without mutual coupling ($p_{\rm woc}$) included between particles. The incident field has $E^{\rm inc} = 1$ V/m and $\phi^{\rm inc} = 90°$.

Surprisingly, it is observed that $\varepsilon_{r,\,\rm eff}$ for the square cylinders in Fig. 2 nearly exactly coincides with the MG curve regardless of the volume fraction, which can reach a maximum of 1 for this lattice. In Fig. 3 it is observed that $\varepsilon_{r,\,\rm eff}$ for the simple cubic lattice of cubes is very close to the MG curve, though not as close as the 2-D lattice of square cylinders. Lattices of dielectric particles rather than conducting ones also produced similar closeness in $\varepsilon_{r,\,\rm eff}$ [8]. The MG formula is often used to predict the static or quasi-static effective permittivity of spherical particles with little mutual interaction. However, it is also known that the MG solution is the lower bound for the static effective permittivity of any isotropic two-phase mixture given that the inclusion permittivity is larger than that of the host [12].

The coincidence of the square cylinder data in Fig. 2 (and to a lesser degree in the cube data of Fig. 3) might lead one to conclude that there is little mutual interaction between the particles. This is not true, however. To illustrate this, shown in Fig. 4 is the surface charge density on a square conducting cylinder over a wide range of volume fraction f. At low volume fraction ($f = 0.1$) the mutual interaction between the inclusions is small and the edge effect is very prominent in Fig. 4 and largely dominates the ρ_s behavior. When the volume fraction becomes very large ($f = 0.9$) and the mutual interaction is significant, however, the interaction of edges (and corners in 3-D) between adjacent particles will combine to reduce these edge effects, which is clearly shown in Fig. 4.

In Fig. 5 we compute $p_{\rm wc}/p_{\rm woc}$ which is the ratio of the electric dipole moments of particles in a 2-D square lattice when including mutual coupling between particles ($p_{\rm wc}$) and without ($p_{\rm woc}$). This family of curves was generated for the class of cylinders we define as the "rounded square" cylinder shown in the key of Fig. 2. In Fig. 5, various ratios b/a are chosen from one to zero and the ratio $p_{\rm wc}/p_{\rm woc}$ is plotted up to the maximal f possible for that particle shape.

All of the curves in Fig. 5 enumerate how the particle dipole moments are affected by mutual coupling as a function of volume fraction. It is apparent from this figure that for circular cylinders, the ratio $p_{\rm wc}/p_{\rm woc}$ starts at one and monotonically increases as f increases. Conversely, for square cylinders this ratio always monotonically decreases from one. Therefore, we see that the circular cross section always causes a "dielectric enhancement," which is a familiar conclusion, since the ratio $p_{\rm wc}/p_{\rm woc}$ is greater than one for all volume fractions. For the square cross section, however, there is only a decrease in $p_{\rm wc}/p_{\rm woc}$ as f increases. Consequently, rather that observing a dielectric enhancement as with circular cylinders, we observe for square cylinders a "dielectric reduction" due to mutual coupling. This mutual coupling is so strong that the minimal amount of polarization per unit volume is attained since in Fig. 2, $\varepsilon_{r,\rm eff}$ is equal to the MG results for $b/a = 0$.

For other rounded-square cylinder shapes, the data in Fig. 5 first show a decrease in $p_{\rm wc}/p_{\rm woc}$ at low f and then an increase as f approaches its maximum. At certain f, this ratio can be unity (for example, see the $b/a = 0.75$ and 0.5 curves) indicating that the dipole moment at these special volume fractions is the same with or without mutual coupling. Nevertheless, we have observed that the surface charge density is very different with and without mutual coupling, as expected.

The last observation from Fig. 5 is that *reduction* of the particle dipole moment with respect to the noninteraction solution is smaller for all rounded-square cylinders compared to the square ($b/a = 0$). Consequently, $\varepsilon_{r,\rm eff}$ is then larger than the MG solution, which is also illustrated in the $b/a = 2/3$ and 1 curves in Fig. 2, for example.

V. Measurement of Effective Conductivity

The dielectric reduction afforded by interacting particle edges and corners reported in the last section is an intriguing phenomenon and one that, to our knowledge, has not been previously recorded in the literature. To provide additional evidence for this phenomenon, we have constructed the measurement apparatus shown in Fig. 6, which is used to measure the relative quasi-static conductivity for a simple cubic lattice of highly conductive cubes. (For quasi-static comparisons, the relative effective conductivity and permittivity will be equivalent quantities since the electric scalar potential in both problems satisfies Laplace's equation with similar boundary conditions [13].) The top and bottom plates shown in the photograph are made from brass while the box is made from Lexan. When the box is filled completely with a moderately conductive fluid and with an applied voltage between the two brass plates, these two surfaces impose *odd* boundary conditions on the electrostatic scalar potential interior to the apparatus. Conversely, the Lexan box—being essentially a nonconductor—imposes *even* boundary conditions on the potential. Consequently, the interior of the apparatus in Fig. 6 forms one-eighth of a unit cell in a simple cubic lattice. Such an apparatus is similar to that used

Fig. 6. Photograph of the conducting cube lattice apparatus for measuring quasi-static effective conductivity. The upper and lower plates as well as the cube are brass. The four-sided box is Lexan. For sample #2 shown above, the measured volume fraction was $f = 0.1952 \pm 0.0005$, as listed in Table I.

TABLE I
Measured Volume Fraction f and Effective Quasi-Static Relative Conductivity $\sigma_{r,\rm eff}$ at 80 kHz for the Cube Apparatus Shown in Fig. 6. The Averages and Uncertainties are the Result of Ten Separate Measurements for f and 16 Separate Measurements for $\sigma_{r,\rm eff}$

Sample #	$f\,(\times 100)^*$	$\sigma_{r,\rm eff}$
1	9.78 ± 0.04	1.40 ± 0.01
2	19.52 ± 0.05	1.88 ± 0.02
3	29.31 ± 0.08	2.46 ± 0.03
4	39.09 ± 0.10	3.21 ± 0.03
5	48.85 ± 0.12	4.21 ± 0.05
6	58.65 ± 0.15	5.67 ± 0.08
7	68.42 ± 0.17	7.99 ± 0.11
8	78.19 ± 0.18	12.4 ± 0.2
9	88.14 ± 0.20	24.0 ± 0.5
10	93.04 ± 0.27	41.1 ± 1.1
11	95.6 ± 0.3	67.2 ± 2.1

* With $f = V_c/V_b$, then $|df| = |dV_c/V_b| + |V_c dV_b/V_b^2|$ where $dV = V(dL/L + dW/W + dH/H)$, $V = LWH$, V_c is the brass cube volume, and V_b is the empty Lexan box volume.

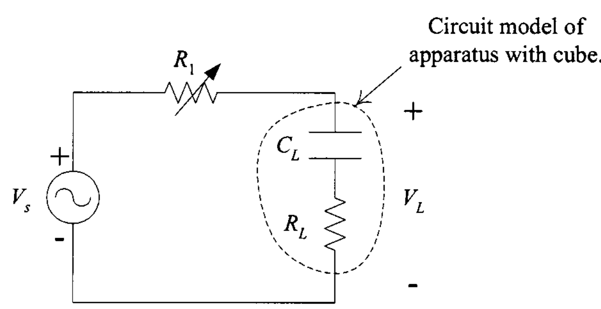

Fig. 7. Equivalent quasi-static circuit model for the experimental measurements of $\sigma_{r,\rm eff}$ using the apparatus in Fig. 6. The effects of the brass plates, brass cube, and Lexan box are modeled by the series combination of C_L and R_L.

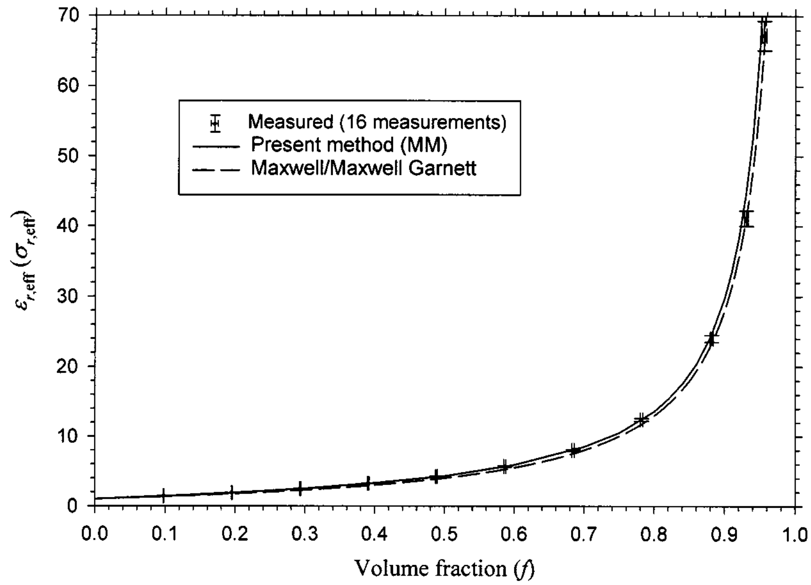

Fig. 8. Predicted quasi-static effective permittivity and measured effective conductivity for a simple cubic lattice of conducting cubes. The measurements were performed at 80 kHz. Error bars indicate one standard deviation in both $\sigma_{r,\,\text{eff}}$ and volume fraction.

by McKenzie *et al.* in their measurements for lattices of spheres [14].

Eleven Lexan boxes were constructed, each of different size to vary the volume fraction of the lattice, while using only one high-precision brass cube. The resulting measured volume fractions of the 11 samples are listed in Table I. Highly precise machining of the brass cube and plate faces as well as the Lexan boxes (within a few thousandths of an inch) was necessary to achieve the small deviations in volume fraction as shown in this table (as well as achieving a watertight fit). For example, the brass cube was found to have dimensions 1.985 $\pm$ 0.0006 in, 1.984 $\pm$ 0.0006 in, and 1.985 $\pm$ 0.0013 in, which were obtained from ten measurements for each of the three dimensions.

The equivalent low-frequency circuit model for this apparatus is shown in Fig. 7. When filled with water and the function generator attached to the two plates, the apparatus electrically appears as a capacitor C_L in series with a resistance R_L. For our measurements, the sinusoidal frequency 80 kHz was chosen to be high enough that $X_c = 1/\omega C_L \ll R_1 + R_L$ so that there was no appreciable phase shift in V_L and V_s. These capacitive effects were actually only noticeable at high volume fraction where the top of the cube was very close to the plate. Such a frequency also avoids possible frequency variations in $\sigma_{r,\,\text{eff}}$ as reported in [14] and [15].

The effective conductivity of the lattice is determined from the ratio of two measurements of R_L. In the first case, the cube is removed from the box, the box is filled with tap water, and the voltage $V_{L,\,\text{empty}}$ is measured. The effective resistance can be easily computed as

$$R_{L,\,\text{empty}} = \frac{R_1}{V_s/V_{L,\,\text{empty}} - 1}. \tag{10}$$

Next, the cube is inserted, the box is filled again with tap water, and the new effective load resistance $R_{L,\,\text{cube}}$ is computed from (10). Forming the ratio of these quantities yields the effective conductivity of the lattice of conducting cubes (relative to the conductivity of the fluid inside the box) as

$$\sigma_{r,\,\text{eff}} = \frac{R_{L,\,\text{empty}}}{R_{L,\,\text{cube}}}. \tag{11}$$

The results of these conductivity measurements are listed in Table I. The average and standard deviation of these measurements are the result of 16 measurements each separated by a disassembly of the apparatus and using different R_1 values ranging from 50 to 500 Ω.

Additionally, these measured $\sigma_{r,\,\text{eff}}$ are plotted in Fig. 8. Two other curves are also shown in this figure. These are the $\varepsilon_{r,\,\text{eff}}$ predicted using our MM solution and the MG solution as shown previously in Fig. 3. The curve of our computed $\varepsilon_{r,\,\text{eff}}$ passes through all of the error boxes centered at each measurement point for $\sigma_{r,\,\text{eff}}$, thus confirming the accuracy of our method for computing effective permittivity for lattices of complex-shaped particles described in Sections II and III.

VI. Conclusion

The effects of inclusion shape on the quasi-static effective permittivity of periodic composites containing complex-shaped conducting particles have been investigated using a simple and accurate moment method based technique. The numerical results showed that, although large mutual interaction exists between particles, lattices of square cylinders (2-D), and cubes (3-D) produce nearly the minimal amount of polarization per unit volume. Consequently, such complex composite materials can be designed with good accuracy using the simple MG formula even though there may exist extremely large coupling between the inclusions. To our knowledge, this interesting phenomenon has not been previously reported in the literature.

This methodology could be applied to microwave structures (high dielectric capacitors, substrates) where the quasi-static effective permittivity of composites must be accurately known.

Our analysis was verified experimentally with measurements of the effective conductivity from an apparatus that simulates an infinite simple cubic lattice of highly conducting cubes.

ACKNOWLEDGMENT

The assistance of T. Fleming with the design and construction of the experimental apparatus of Fig. 6 is gratefully acknowledged.

REFERENCES

[1] J. Lin, N. Masaaki, A. Tsukune, and M. Yamada, "Ta2O2 thin films with exceptionally high dielectric constant," *Appl. Phys. Lett.*, vol. 74, no. 16, pp. 2370–2372, 1999.

[2] B. Sareni, L. Krähenbühl, A. Beroual, A. Nicolas, and C. Brosseau, "A boundary integral equation method for the calculation of the effective permittivity of periodic composites," *IEEE Trans. Magn.*, vol. 33, pp. 1580–1583, Mar. 1997.

[3] W. C. Chew, *Waves and Fields in Inhomogeneous Media*. New York: Van Nostrand, 1990.

[4] R. C. McPhedran and N. A. Nicorovici, "Effective dielectric constant of arrays of elliptical cylinders," *Physica A*, vol. 241, pp. 173–178, 1997.

[5] K. W. Whites and F. Wu, "Computing the effective permittivity for a mixture of spherical particles," in *Bianisotropics'98 7th Int. Conf. Complex Media*, Braunschweig, Germany, June 3–6, 1998, pp. 285–288.

[6] J. Van Bladel, *Singular Electromagnetic Fields and Sources*. Oxford, U.K.: Clarendon, 1991.

[7] K. W. Whites, "Permittivity of a multiphase and isotropic lattice of spheres at low frequency," *J. Appl. Phys.*, vol. 88, no. 4, pp. 1962–1970, 2000.

[8] F. Wu and K. W. Whites, "Quasi-static effective permittivity of periodic composites containing complex shaped dielectric particles," *IEEE Trans. Antennas Propagat.*, vol. 49, pp. 1174–1182, Aug. 2001.

[9] ——, "Computation of static effective permittivity for a multiphase lattice of cylinders," *Electromagnetics*, vol. 21, no. 2, pp. 97–114, 2001.

[10] R. C. McPhedran and D. R. McKenzie, "The conductivity of lattices of spheres: I. The simple cubic lattice," *Proc. R. Soc. Lond. A, Math. Phys. Sci.*, vol. 359, pp. 45–63, 1978.

[11] J. C. Maxwell, *A Treatise on Electricity and Magnetism*, 3rd ed. New York: Dover, 1954.

[12] Z. Hashin and S. Shtrikman, "A variational approach to the theory of the effective magnetic permeability of multiphase materials," *J. Appl. Phys.*, vol. 33, no. 10, pp. 3125–3131, 1962.

[13] S. Ramo, J. R. Whinnery, and T. Van Duzer, *Fields and Waves in Communication Electronics*, 3rd ed. New York: Wiley, 1994.

[14] D. R. McKenzie, R. C. McPhedran, and G. H. Derrick, "The conductivity of lattices of spheres: II. The body centred and face centred cubic lattices," *Proc. R. Soc. Lond. A, Math. Phys. Sci.*, vol. 362, pp. 211–232, 1978.

[15] R. E. Meredith and C. W. Tobias, "Resistance to potential flow through a cubical array of spheres," *J. Appl. Phys.*, vol. 31, no. 7, pp. 1270–1273, 1960.

Keith W. Whites (S'84–M'86–SM'99) was born in Huron, SD. He received the B.S.E.E. degree from the South Dakota School of Mines and Technology, Rapid City, in 1986 and the M.S. and Ph.D. degrees from the University of Illinois, Urbana/Champaign, in 1988 and 1991, respectively.

In 1986, he was a Graduate Summer Assistant at Sandia National Laboratories, Livermore, CA, and during 1987–1988, he was a Research Assistant with the U.S. Army CERL, Champaign, IL. From 1988 to 1991, he held various fellowships and assistantships at the University of Illinois. He was an Assistant and later an Associate Professor in the Department of Electrical and Computer Engineering, University of Kentucky, from 1991 to 2001. Since 2001, he has been with the South Dakota School of Mines and Technology, where he is currently a Professor and the Steven P. Miller Chair in Electrical Engineering, teaching courses in applied electromagnetics and wireless communications, among other topics. His current research interests include effective media calculations for complex composite materials; electromagnetic interaction with ultralightweight spacecraft, including propulsion and control of solar sails; computational electromagnetics; equivalent boundary condition models; and homogenization of electromagnetics problems.

Dr. Whites was the 1999 recipient of the R.W.P. King Prize Paper Award from the IEEE Antennas and Propagation Society and a recipient of NSF Faculty Early Career Development (CAREER) and Research Initiation Awards. He is a member of Tau Beta Pi and Eta Kappa Nu.

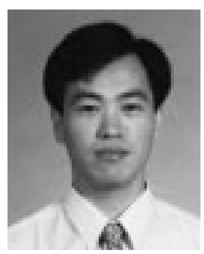

Feng Wu was born in Huangshi, China, in 1971. He received the B.S. and M.S. degrees in physics from Zhejiang University, Hangzhou, China, in 1993 and 1996, respectively. He is currently working toward the Ph.D. degree in the Department of Electrical and Computer Engineering, University of Kentucky, Lexington.

From 1996 to 1997, he was a Lecturer in the Department of Physics, Zhejiang University, where he performed research on electromagnetic properties of composite materials, mainly chiral and omega media. Since August 1997, he has been with the Department of Electrical and Computer Engineering, University of Kentucky. His research interests include effective medium and scattering theory, computational electromagnetics, and numerical algorithms.

Mr. Wu is a member of Eta Kappa Nu.